A Comparative Analysis on Proportional-Integral and Fuzzy-Logic Control Strategies for Doubly-Fed Induction Generators

ANKINEEDU PRASAD PADAMATA[1,*], GUDAPATI SAMBASIVA RAO[2]
[1]Electrical and Electronics Engineering,
Dr. YSR ANU College of Engineering & Technology,
Acharya Nagarjuna University,
Nagarjuna Nagar, Guntur - 522 510, Andhra Pradesh,
INDIA

[2]Department of Electrical & Electronics Engineering,
R.V.R. & J.C. College of Engineering,
Guntur - 522 019, Andhra Pradesh,
INDIA

Corresponding Author

Abstract: - This research investigates superior control methods for optimize the performance of Doubly-Fed Induction Generators in wind energy conversion systems. This proposed work, compares the well-established Proportional-Integral controller, with a Fuzzy Logic controller, known for its effectiveness in managing non-linear systems. To achieve a thorough analysis, this research develops a detailed mathematical model, specifically adopted to the DFIG system. It employs a PI controller for both the rotor-side and grid-side converters of the DFIG system. To enhance performance, a Fuzzy Logic controller is introduced to replace the PI controller, based on real-time operating conditions and gain values. Extensive simulations evaluate rigorously various performance metrics of the DFIG system under different control strategies. This analysis provides valuable insights to guide the selection of optimal control techniques, for wind energy systems using DFIGs. The analysis contributes to advancements in reliability, and efficiency for DFIG-based wind-energy systems, furthering the development of sustainable energy solutions.

Key-Words: - Control strategies, DFIGs, PI controller, Fuzzy-Logic Controller (FLC), mathematical model, wind energy systems, performance metrics, efficiency.

Received: April 9, 2023. Revised: February 4, 2024. Accepted: March 17, 2024. Published: April 16, 2024.

1 Introduction

There has been a significant rise in interest surrounding wind energy conversion systems. Amidst the array of wind power generation techniques, DFIG distinguishes itself with its enhanced energy transfer capability, cost efficiency, and, adaptable control features, [1].

Wind turbines, devices converting wind kinetic energy to electrical energy, come in various types- “horizontal”, “vertical”, “constant” and “adjustable” speed generator, and varying blade numbers, [2]. DFIG, a variable-speed generator, minimizes losses by recuperating slip power in both sub-synchronous and hyper-synchronous modes, enhancing efficiency across a broad range of wind speeds. Achieving this involves a tandem AC-DC-AC converter on the rotor circuit. Additionally, the stator's direct grid connection ensures the converter handles only a minimal portion of overall output power (approximately±30%), eliminating the necessity of expensive full-scale converter, [3].

Diverging from traditional generators, DFIG incorporates a sequence “voltage-source converter” for the wound-rotor. The inclusion of converters with feedback, specifically the in rotor-side, and grid-side, enhances DFIG's control capabilities, and stability, surpassing those of other generators.

A prevalent DFIG control technique is vector control, employed on the “RSC”, for independent control of real. and responsive power. This can be achieved by decoupling the rotor currents, into two components, akin direct, and quadrature, managing the real, and responsive power respectively, [4].

The control strategy, established in the traditional PI control-technique, involves controllers for P_{sref}, V_{sref}, V_{dcref}, and Q_{sref}, ensuring optimal power monitoring, stator terminal voltage-regulation, DC voltage level, and responsive power level at GSC, [5]. Despite conventional use of PI controllers, their limitations in robustness and tuning have prompted exploration of alternative control methods, [6].

Studies have explored the dynamic behavior of DFIG, from transient stability models, [7], to detailed grid-connected DFIG models, [8]. Modal analysis, addressing changes in modal characteristics under various operating scenarios, and system specifications, has also been explored, [9]. Prior works on delink control of real, and responsive power for DFIG, have been illustrated, [10].

In this paper, by recognizing PI controller shortcomings, a Fuzzy Logic Controller (FLC) for DFIG is proposed. Fuzzy control has found application in various wind-turbine controls, comprising of swift control, pitch-control, MPPT, and extracted power control, [11], [12], [13], [14].

The fuzzy logic approach provides a non-linear, model-free control approach, suitable for coordinated RSC, and GSC control in DFIG system. While “Mamdani-type” controllers may have limitations, a “Takagi-Sugeno” (TS) type fuzzy controller provides a broader scope of control gain adjustment. It is emphasized the implementation of TS fuzzy controllers for regulating real power output, and DC capacitor voltage in DFIG, demonstrating its effectiveness in suppression of rotor speed oscillations, and regulating DC voltage fluctuations, [15].

In line with current grid codes, wind farms must withstand system faults, necessitating ability to ride through faults. The effectiveness of TS-fuzzy controllers on DC voltage variation, and rotor speed oscillations, evaluating the impact on improving the system's fault ride-through capability, [16].

The implementation of a tandem connected AC-DC-AC converter for DFIG's integration into the grid underscores the importance of power electronic converters. Operating with a fraction of the overall system power, these converters hold promise for minimizing losses in contrast to direct-driven synchronous generators, [17]. Within this investigation, two controller types are introduced: proportional-integral (PI) for governing real power through torque control and Fuzzy-PI for managing speed control.

2 System Model

2.1 DFIG Model

Being the variable-speed nature of the DFIG, its stator connects straightforwardly to the grid, via an isolation-transformer, delivering the majority of power. Simultaneously, the rotor links via a tandem AC-DC-AC converter, enabling slip power recuperation. The converter in this study includes two tandem VSCs (1-RSC and 2-GSC) with a capacitor establishing a DC bus. With an effective control approach, the tandem converters facilitate mutual power transmission, governing real, and responsive power, [18].

2.2 Rotor Side Controller

During the initial phase, rotor current references "i_{qr_ref}", and "i_{dr_ref}" are computed based on the real (P_{sref}), and responsive (Q_{sref}) reference powers. These are then compared with i_{qr_ref} and i_{dr_ref}. Differences are computed using two PI controllers, generating dq reference voltages, $\hat{v}$ = (v_{dr_ref}, v_{qr_ref}). These are transformed to the rotor's synchronous reference and applied through a PWM modulator, [19]. The control system equations are given in (1) to (5).

$$i_{dr\_ref} = \frac{-2L_s Q_{s\_ref}}{3v_s L_m} + \frac{\lambda_s}{L_m} \tag{1}$$

$$i_{qr\_ref} = \frac{-2L_s P_{s\_ref}}{3v_s L_m} \tag{2}$$

$$\begin{aligned} v_{dr\_ref} &= (i_{dr\_ref} - i_{dr})(k_p + k_{pi}/s) + D_{dr} \\ v_{qr\_ref} &= (i_{qr-ref} - i_{qr})(k_p + k_{pi}/s) + D_{qr} \end{aligned} \tag{3}$$

$$D_{dr} = -\omega_s \left(L_r + L_m^2/L_s \right) i_{qr} \tag{4}$$

$$D_{qr} = \omega_s \left(L_r - L_m^2/L_s \right) i_{dr} + (L_m/L_s)\, \lambda_s) \tag{5}$$

Where D_{dr} and D_{qr} symbolize coupling residues.

2.3 Controller Gain Design for i_{dqr}

In this article, a current loop model is utilized to determine the appropriate gains of the PI controller, simplifying the power loop used [20]. This approach reduces the system's complexity, as it employs the direct power control technique.

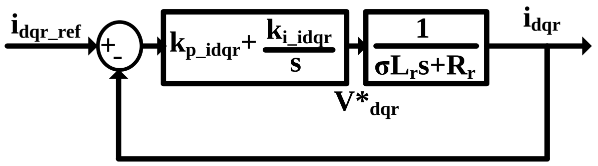

Fig. 1: PI Controller for i_{dqr}

The PI control scheme for the control current i_{dqr} is shown in Figure 1. The gain k_{p_idqr} is described by,

$$k_{p\_idqr} = \frac{\sigma L_r}{\omega_{nr}} \quad (6)$$

$$k_{i\_idqr} = \frac{R_r}{T_{cr}} \quad (7)$$

Where ω_{nr}= Natural angular frequency
$\omega_{nr} = 100/T_{cr}$
σ = Leakage factor
L_r= Stator-referred rotor inductance
R_r= Stator-referred rotor resistance
T_{cr}= Rotor Time constant
$T_{cr} = \frac{\sigma L_r}{R_r}$

2.4 Speed Controller Gains

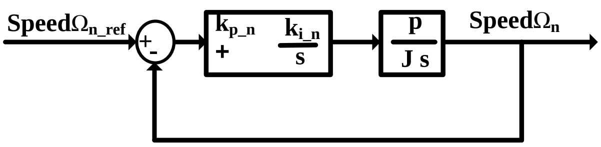

Fig. 2: PI controller implemented for Speed control

The Figure 2 shows the speed control loop with PI controller which is implemented in the DFIG system. The proportional constant for speed controller is given by the following equations:

$$k_{p\_n} = 2\omega_{nn}\left(\frac{J}{P}\right) \quad (8)$$

$$k_{i\_n} = \omega_{nn}^2\left(\frac{J}{P}\right) \quad (9)$$

Where $\omega_{nn} = \frac{1}{\tau_n}$ = Natural angular frequency (τ_n= 0.05)
J= Moment of Inertia
p= Pair of poles

2.5 PI Controller in GSC

The voltages on the grid side in the dq coordinate framework are expressed as follows:

$$v_{dg\_ref} = \left(i_{dg\_ref} - i_{dg}\right) + \left(k_{pg} + k_{ig}/s\right) + e_q \quad (10)$$

$$v_{qg\_ref} = \left(i_{qg\_ref} - i_{qg}\right) + \left(k_{pg} + k_{ig}/s\right) + e_d \quad (11)$$

$$e_q = -\omega_{ng}\, L_g i_{qg} \quad (12)$$

$$e_d = -\omega_{ng}\, L_g i_{dg} \quad (13)$$

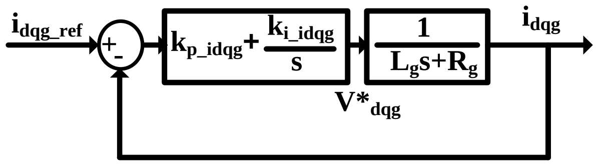

Fig. 3: PI Controller implemented in PI Controller

The Figure 3 shows the grid currents control loop in GSC. Here the gains k_{p_idqg} and k_{i_idqg} are described by the following equations:

$$k_{p\_idqg} = 2\omega_{ng}L_g - R_g \quad (14)$$

$$k_{i\_idqg} = \omega_{ng}^2 L_g \quad (15)$$

Where $\omega_{ng} = 2\pi f$
L_g = Inductance of the grid-filter
R_g = Resistance of the grid-filter
$T_{cg} = \frac{L_g}{R_g}$

2.6 PI Controller in DC Link

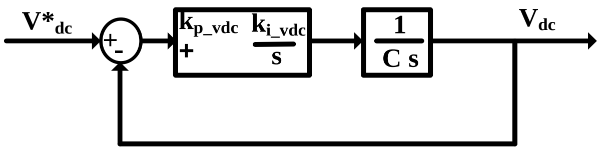

Fig. 4: PI controller implemented in DC link

The Figure 4 shows the PI Controller implemented in DC link. The control equation can be expressed as follows. Here the gains k_{p_vdc}, and k_{i_vdc} can be described by the equations (17) and (18).

$$C\frac{dV_{dc}}{dt} = i_{dc} - \frac{1.5}{V_{dc}}\left(V_{dg}\, i_{dg} + V_{dg}\, i_{dg}\right) \quad (16)$$

$$k_{p\_vdc} = 2C\,\omega_{nvdc} \quad (17)$$

$$k_{i\_vdc} = C\,\omega_{nvdc}^2 \quad (18)$$

It is observed that the DC link potential can be regulated by adjusting the real power. Additionally, the DC bus potential is influenced by the external current i_{dc} flowing into the converter's DC bus.

3 Fuzzy Controller

The Fuzzy Logic Controller (FLC) is recognized for its ability to adapt to nonlinear systems through the incorporation of human knowledge and expertise in decision-making. This proposed investigation emphasizes on implementing the "FLC" due to its "robustness", and "effectiveness" in managing nonlinear systems. "Mamdani" model is opted due to its capacity to retain Optimization as emphasized, [21]. Implementing this controller would be a straightforward role. Separate FLC controllers are employed in conjunction with vector control scheme of the RSC. First is designated to regulate the "i_{dr}" which corresponds to the orientation of the stator flux vector in space. The arrangement ensures that the i_{dr} is directly related to the produced responsive power. Second is employed for regulation of the "i_{qr}" which is directly related to the evolved electromotive-torque. This configuration enables speed-regulation, and accordingly the control over produced real power, [22]. The architecture diagram of FLC is shown in Figure 5.

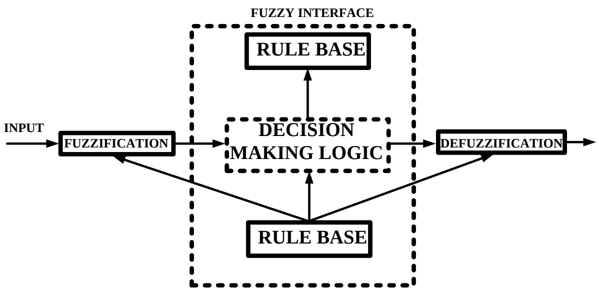

Fig. 5: Architecture of FLC

3.1 Fuzzy Controller to DFIG

Fuzzy theory constitutes a numerical control algorithm founded on principles derived from Fuzzy set-theory, Fuzzy-linguistic-variables, and Fuzzy logic. Adjustments are made to the rules and membership functions in a manner that enhances the efficacy of the FLC. The membership functions are configured to position them in proximity to the zero region, aiming to enhance control performance. Conversely, positioning them farther from the zero region contributes to a quicker control response.

Enhancements in performance can be achieved by modifying both the rules and membership functions. Observing the response characteristics such as rise time, settling time, and maximum overshoot can be accomplished by systematically varying the values of " k_p" & "k_i" across multiple iterations. The two inputs, error and change in error, are characterized by seven variables each, including: Tiny (T), Small (S), Petite (P), Normal (N), Grande (G), Large (L), Enormous (E) so as to form a (7X7) matrix for the Fuzzy rules as shown in Table 1.

Table 1. Rule base for MF in FLC

e_r/rs	T	S	P	N	G	L	E
T	TT	TS	TP	TN	TG	TL	TE
S	ST	SS	SP	SN	SG	SL	SE
P	PT	PS	PP	SN	SG	SL	SE
N	NT	NS	NP	NN	NG	NL	NE
G	GT	GS	GP	GN	GG	GL	GE
L	LT	LS	LP	LP	LG	LL	LE
E	ET	ES	EP	EN	EG	EL	EE

The gain attributes of the PI controller are subjected to reconciliation through methods such as trial and error or by employing the Ziegler-Nichols tuning technique. The adjustment of the values for " k_p" & "k_i" is carried out based on the Fuzzy membership functions and rules implemented, thereby constituting a Fuzzy controller. The rule bases for tuning the values of " k_p" & "k_i" are specified in Tables.

Manually designing the Fuzzy Logic Controller (FLC) involved employing an iterative approach. Incorporating "membership-functions (MFs)" with interims, that vary in span, are essential, with the narrow interim approaching zero, to enhance accuracy. In this framework, the suggested RSC block utilizes a simple inherent speed regulation approach. This strategy utilizes the recorded rotor speed to generate a reference electromotive-torque. The reference torque is intended to utilize in the " i_{qr}" control, [19].

3.2 Fuzzy "i_{dr}" Control

In the control of DFIG, setting the reference to zero is a typical practice, as implemented in this paper. Indeed, the adjustment is made to diminish the required rotor-currents, effectively restricting the dimensioning of the rotor-windings, [23]. This aspect similarly enables the restriction of the control over responsive power-generation exclusively to the Grid Side Converter. The employed regulator utilized a Mamdani fuzzy-system with one input and one output, featuring 7 MFs for incorporating both input and output variables, [24].

3.3 Fuzzy "i_{qr}" Control

The system takes the error (er) as input and produces the Control parameter (Ctr) as its output. The details of MFs and rules are outlined in Figure 6, Table 2 and Table 3.

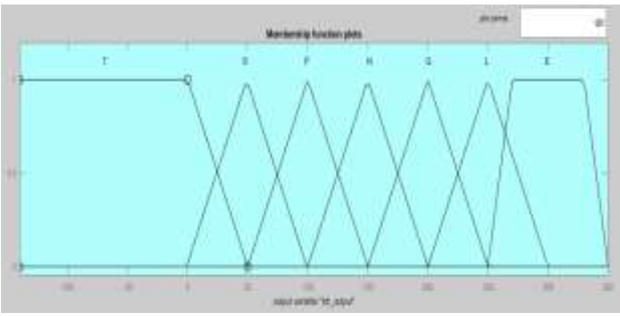

Fig. 6: MF of i_{dr} for FLC

Table 2. $\mathbf{i_{dr}}$ MF Types and Range

	MF	Type	Range
i_{dr} _e_r	T	Trapezoidal	[-50 -50 0 50]
	S	Triangle	[0 50 100]
	P	Triangle	[50 100 150]
	N	Triangle	[100 150 200]
	G	Triangle	[150 200 250]
	L	Triangle	[200 250 300]
	E	Trapezoidal	[230 270 320 350]
Ctr_v_{dr}	T	Trapezoidal	[-140 -140 0 50]
	S	Triangle	[0 50 100]
	P	Triangle	[50 100 150]
	N	Triangle	[100 150 200]
	G	Triangle	[150 200 250]
	L	Triangle	[200 250 300]
	E	Trapezoidal	[250 270 330 350]

Table 3. $\mathbf{i_{dr}}$ Rule Table

i_{dr} _e_r	T	S	P	N	G	L	E
Ctr_v_{dr}	T	S	P	N	G	L	E

Figure 7 shows the MF of i_{dg} for FLC and Table 4 and Table 5, describes MF range and rule base. Similarly, the FLC and rule base can be implemented for i_{qg}.

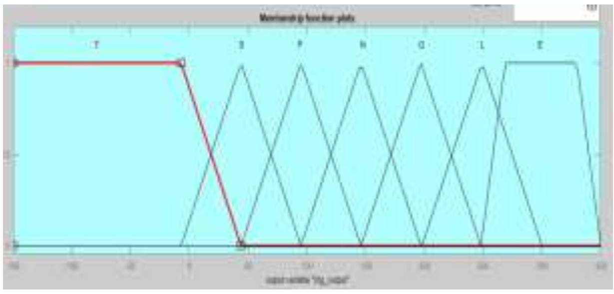

Fig. 7: MF of i_{dg} for FLC

Table 4. $\mathbf{i_{dg}}$ MF Types and Range

	MF	Type	Range
i_{dg}_e_r	T	Trapezoidal	[-160 -160 -82 -31]
	S	Triangle	[-96.25 -32.5 31.25]
	P	Triangle	[-32.5 31.25 95]
	N	Triangle	[31.25 95 158.8]
	G	Triangle	[95 158.8 222.5]
	L	Triangle	[158.8 222.5 286.2]
	E	Trapezoidal	[229 268.7 312 350]
Ctr_v_{dg}	T	Trapezoidal	[-150 -150 -7 43]
	S	Triangle	[-7.143 43.88 94.9]
	P	Triangle	[43.88 94.9 145.9]
	N	Triangle	[94.9 145.9 196.9]
	G	Triangle	[145.9 196.9 248]
	L	Triangle	[197.8 248.9 299.9]
	E	Trapezoidal	[248 268 329 350]

Table 5. $\mathbf{i_{dg}}$ Rule Table

i_{dg} _e_r	T	S	P	N	G	L	E
Ctr_v_{dg}	T	S	P	N	G	L	E

Figure 8 describes MF of Speed_e_r for FLC and and Table 6 and Table 7, describes MF range and rule base.

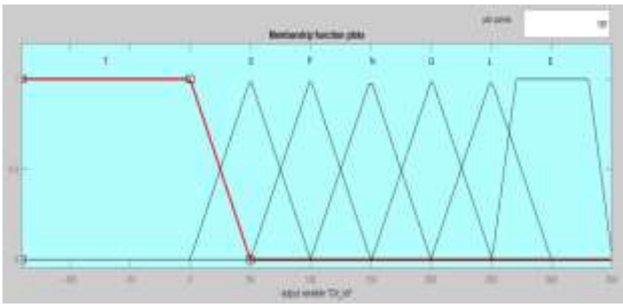

Fig. 8: MF of Speed_e_r for FLC

Table 6. Speed MF Types and Range

	MF	Type	Range
Speed_e_r	T	Trapezoidal	[-50 -50 0 50]
	S	Triangle	[0 50 100]
	P	Triangle	[50 100 150]
	N	Triangle	[100 150 200]
	G	Triangle	[150 200 250]
	L	Triangle	[200 250 300]
	E	Trapezoidal	[230 270 320 350]
Ctr_i_{dr}	T	Trapezoidal	[-140 -140 0 50]
	S	Triangle	[0 50 100]
	P	Triangle	[50 100 150]
	N	Triangle	[100 150 200]
	G	Triangle	[151 201 251]
	L	Triangle	[200 250 300]
	E	Trapezoidal	[250 270 330 350]

Table 7. Speed_e_r Rule Table

Speed_e_r	T	S	P	N	G	L	E
Ctr_i_{dr}	T	S	P	N	G	L	E

4 Comparative Analysis

The wind speed is held at 8m/s for the first 2 seconds. From 2 to 3 seconds, it increases to 9m/s. The wind speed remains consistently at 10m/s from 3 to 4 seconds. Between 4 and 5 seconds, the wind speed is set at 11m/s. From 5 to 6 seconds, the wind speed is sustained at 12m/s, and from 6 to 7 seconds, it further increases to 13m/s shown in Figure 9.

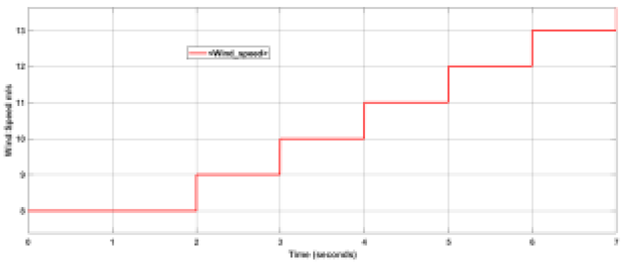

Fig. 9: Wind speed response

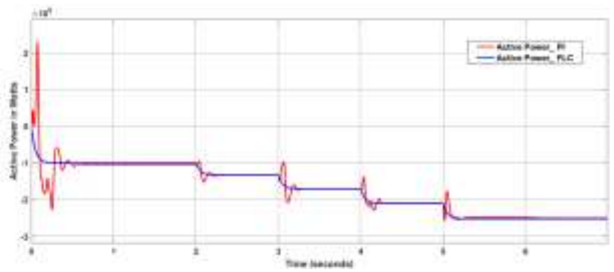

Fig. 10: Active Power extracted with DFIG

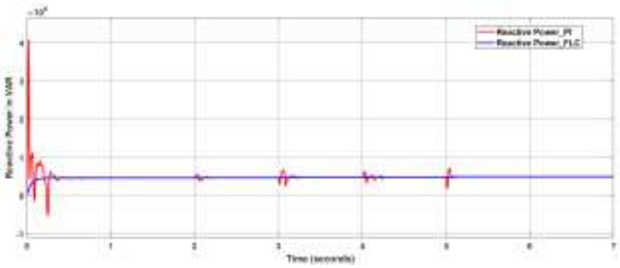

Fig. 11: Reactive Power Consumed by the DFIG

The power extraction is analyzed in both cases, namely, with a PI controller and a Fuzzy controller. The Figure 10 shows the active power extracted from the wind and Figure 11 shows reactive power consumed from the grid. In the context of reference tracking ability, both FLC, and PI controller demonstrate comparable performance, exhibiting fluctuations of in steady state. Notably, the FLC exhibits a faster settling time to the reference, analyzed to the PI controller. This implies that the FLC achieves the desired reference value more rapidly and with reduced oscillations, illustrates its superior transient response characteristics.

The faster settling time of the FLC suggests a more agile and responsive control mechanism, particularly beneficial in scenarios where quick and accurate adjustments to the reference are crucial. Although both controllers, achieve identical tracking abilities, the nuanced disparity in settling-time emphasizes the efficiency of Fuzzy-Logic Control in promptly attaining, and, sustaining the desired reference. This distinction emphasizes Fuzzy-Logic Control's expertise at quickly reaching, and, maintaining the desired reference, particularly when compared to the PI controller. Table 8 shows the power extracted with PI and FLC. The machine name plate details are provided in Table 9.

Table 8. Active Power extracted from wind

Wind	DFIG	
m/s	PI-Active Power in KW	FLC- Active Power in KW
8	104	100
9	137.5	132.5
10	170.5	170
11	208.75	209.25
12	247.5	251.25
13	250.25	251.25

Table 9. DFIG name plate details:

Power(P)	250 KW
Stator Voltage (V_s)	400 V
Stator Current (I_s)	370 A
Rotor Voltage (V_r)	400 V
Poles pair(p)	2
Frequency(f)	50Hz
Rotor speed (ω)	1500 rpm/157.1 rad/s
DC Bus Voltage (V_{dc})	600V

5 Conclusions

The paper presents a control-system designed for a DFIG-based wind turbine, employing vector control techniques. The study incorporates a comparative analysis between a Mamdani FLC, and a PI controller. The results indicate that, the FLC exceeds the PI controller, exhibiting a quicker, and more precise response. The implementation of FLC results, in a higher electromagnetic torque reference, causing a slightly elevated rotational rotor speed in comparison to the PI controller.

This outcome indicates that, the improved dynamic response, and efficiency of the FLC within the structure of DFIG-based wind turbine control. The paper recognizes the potential for further advancements, emphasizing the importance of exploring smarter control methods for improved tuning of the FLC.

This suggests a continuous interest in refining, and enhancing, the control strategy to achieve better performance, and maximize potential energy yield in DFIG-based wind turbine systems.

References:

[1] M. W. Rahman, K. Velmurugan, M. S. Mahmud, A. Al Mamun and P. Ravindran, "Modeling of a stand-alone Wind-PV Hybrid Generation System Using (MATLAB/SIMULINK)," *2021 International Conference on Computing, Communication, and Intelligent Systems (ICCCIS)*, Greater Noida, India, 2021, pp. 1000-1006, doi: 10.1109/ICCCIS51004.2021.9397194.

[2] B. Spichartz, K. Günther and C. Sourkounis, "New Stability Concept for Primary Controlled Variable Speed Wind Turbines Considering Wind Fluctuations and Power Smoothing," in *IEEE Transactions on Industry Applications*, vol. 58, no. 2, pp. 2378-2388, March-April 2022, doi: 10.1109/TIA.2022.3144650.

[3] C. Z. El Archi, T. Nasser, A. Essadki and J. Alvarado, "Real Power Control: MPPT and Pitch Control in a DFIG Based Wind Turbine," *2020 3rd International Conference on Advanced Communication Technologies and Networking (CommNet)*, Marrakech, Morocco, 2020, pp. 1-6, doi: 10.1109/CommNet49926.2020.9199625.

[4] Abad, Gonzalo, et al. *Doubly fed induction machine: modeling and control for wind energy generation*. John Wiley & Sons, 2011.

[5] L. Saihi, Y. Bakou, F. Ferroudji, B. Berbaoui and L. Djilali, "MPPTF & Pitch Fuzzy Controller of a Wind Turbine System Using DFIG," *2019 1st International Conference on Sustainable Renewable Energy Systems and Applications (ICSRESA)*, Tebessa, Algeria, 2019, pp. 1-6, doi: 10.1109/ICSRESA49121.2019.9182282.

[6] M. N. Uddin, M. S. Arifin and N. Rezaei, "A Novel Neuro-Fuzzy Based Direct Power Control of a DFIG Based Wind Farm Incorporated With Distance Protection Scheme and LVRT Capability," in *IEEE Transactions on Industry Applications*, vol. 59, no. 5, pp. 5792-5803, Sept.-Oct. 2023, doi: 10.1109/TIA.2023.3289441.

[7] A. Dash, A. Behera and D. P. Bagarty, "Modelling Of Doubly-Fed Induction Generator With Variable Wind Speed," 2023 *IEEE 3rd International Conference on Sustainable Energy and Future Electric Transportation (SEFET)*, Bhubaneswar, India, 2023, pp. 1-5, doi: 10.1109/SeFeT57834.2023.10245883.

[8] C. Yi, Z. Ma, Z. Li, P. Song, Y. Zhang and X. Zhang, "Modeling and Stability Analysis of Doubly-fed Induction Generator Based on Impedance Analysis Method for Voltage Source Control," *2022 5th Asia Conference on Energy and Electrical Engineering (ACEEE)*, Kuala Lumpur, Malaysia, 2022, pp. 97-102, doi: 10.1109/ACEEE56193.2022.9851876.

[9] G. P. Prajapat, N. Senroy and I. N. Kar, "Modal analysis of grid connected DFIG with detailed structural modeling of wind turbine," *2017 IEEE Innovative Smart Grid Technologies - Asia (ISGT-Asia)*, Auckland, New Zealand, 2017, pp. 1-6, doi: 10.1109/ISGT-Asia.2017.8378399.

[10] W. K. Ntuli, G. Sharma and M. Kabeya, "A comparative study of DFIG-based wind energy conversion systems with Fuzzy-PID and Fuzzy-logic controllers," *2022 IEEE PES/IAS PowerAfrica*, Kigali, Rwanda, 2022, pp. 1-5, doi: 10.1109/PowerAfrica53997.2022.9905240.

[11] I. Kharchouf, A. Essadki, M. Fdaili and T. Nasser, "Comparative Study of MPPT and Pitch Angle using PI and Fuzzy Logic Controllers," *2018 6th International Renewable and Sustainable Energy Conference (IRSEC)*, Rabat, Morocco, 2018, pp. 1-6, doi: 10.1109/IRSEC.2018.8702882.

[12] M. Kesraoui, S. A. Lagraf and A. Chaib, "Aerodynamic power control of wind turbine using fuzzy logic," *2015 3rd International Renewable and Sustainable Energy Conference (IRSEC)*, Marrakech, Morocco, 2015, pp. 1-6, doi: 10.1109/IRSEC.2015.7455110.

[13] T. K. Mahmoud, Z. Y. Dong and J. Ma, "A Developed Integrated Scheme Based Approach for Wind Turbine Intelligent Control," in *IEEE Transactions on Sustainable Energy*, vol. 8, no. 3, pp. 927-937, July 2017, doi: 10.1109/TSTE.2016.2632104.

[14] M. S. Arifin, M. N. Uddin and W. Wang, "Neuro-Fuzzy Adaptive Direct Torque and

Flux Control of a Grid-Connected DFIG-WECS With Improved Dynamic Performance," in *IEEE Transactions on Industry Applications*, vol. 59, no. 6, pp. 7692-7700, Nov.-Dec. 2023, doi: 10.1109/TIA.2023.3302844.

[15] L. Shanmugam and Y. H. Joo, "Stability and Stabilization for T–S Fuzzy Large-Scale Interconnected Power System With Wind Farm via Sampled-Data Control," in *IEEE Transactions on Systems, Man, and Cybernetics: Systems*, vol. 51, no. 4, pp. 2134-2144, April 2021, doi: 10.1109/TSMC.2020.2965577.

[16] S. Khateri-abri, S. Tohidi and N. Rostami, "Improved Direct Power Control of DFIG Wind Turbine by using a Fuzzy Logic Controller," *2019 10th International Power Electronics, Drive Systems and Technologies Conference (PEDSTC)*, Shiraz, Iran, 2019, pp. 458-463, doi: 10.1109/PEDSTC.2019.8697581.

[17] N. K. S. Naidu and B. Singh, "Grid-Interfaced DFIG-Based Variable Speed Wind Energy Conversion System With Power Smoothening," in *IEEE Transactions on Sustainable Energy*, vol. 8, no. 1, pp. 51-58, Jan. 2017, doi: 10.1109/TSTE.2016.2582520.

[18] J. Ying, X. Yuan, J. Hu and W. He, "Impact of Inertia Control of DFIG-Based WT on Electromechanical Oscillation Damping of SG," in *IEEE Transactions on Power Systems*, vol. 33, no. 3, pp. 3450-3459, May 2018, doi: 10.1109/TPWRS.2018.2801283.

[19] J. H. Park, J. S. Lee and U. M. Choi, "Sinusoidal Third Harmonic Voltage Injection PWM Method for Applying the LCL Filter to Vienna Rectifiers," *2019 10th International Conference on Power Electronics and ECCE Asia (ICPE 2019 - ECCE Asia)*, Busan, Korea (South), 2019, pp. 2272-2277, doi: 10.23919/ICPE2019-ECCEAsia42246.2019.8797309.

[20] S. Hu, G. Zhu and Y. Kang, "Modeling and Coordinated Control Design for Brushless Doubly-Fed Induction Generator-Based Wind Turbine to Withstand Grid Voltage Unbalance," in *IEEE Access*, vol. 9, pp. 63331-63344, 2021, doi: 10.1109/ACCESS.2021.3074528.

[21] J. Liu, Y. Gao, S. Geng and L. Wu, "Nonlinear Control of Variable Speed Wind Turbines via Fuzzy Techniques," in *IEEE Access*, vol. 5, pp. 27-34, 2017, doi: 10.1109/ACCESS.2016.2599542.

[22] S. Krishnama Raju and G. N. Pillai, "Design and Implementation of Type-2 Fuzzy Logic Controller for DFIG-Based Wind Energy Systems in Distribution Networks," in *IEEE Transactions on Sustainable Energy*, vol. 7, no. 1, pp. 345-353, Jan. 2016, doi: 10.1109/TSTE.2015.2496170.

[23] X. Lin, K. Xiahou, Y. Liu and Q. H. Wu, "Design and Hardware-in-the-Loop Experiment of Multiloop Adaptive Control for DFIG-WT," in *IEEE Transactions on Industrial Electronics*, vol. 65, no. 9, pp. 7049-7059, Sept. 2018, doi: 10.1109/TIE.2018.2798566.

[24] Hong Hee Lee, Phan Quoc Dzung, Le Minh Phuong, Le Dinh Khoa and Nguyen Huu Nhan, "A new fuzzy logic approach for control system of wind turbine with Doubly Fed Induction Generator," *International Forum on Strategic Technology 2010*, Ulsan, Korea (South), 2010, pp. 134-139, doi: 10.1109/IFOST.2010.5667902.

Contribution of Individual Authors to the Creation of a Scientific Article (Ghostwriting Policy)

The authors equally contributed in the present research, at all stages from the formulation of the problem to the final findings and solution.

Sources of Funding for Research Presented in a Scientific Article or Scientific Article Itself

No funding was received for conducting this study.

Conflict of Interest

The authors have no conflicts of interest to declare.